Aqueous Solutions of Poly(ethyloxazoline) and Its Lower Consolute Phase Transition

F. P. Chen,* A. E. Ames, and L. D. Taylor

Polaroid Corp., Cambridge, Massachusetts 02139

Received October 9, 1989; Revised Manuscript Received March 26, 1990

ABSTRACT: Poly(2-ethyloxazoline) is a tertiary amide polymer that is completely soluble in water at temperatures below 60 °C, above which the system undergoes a liquid–liquid phase segregation. For M_w = 116 000 and M_w/M_n = 2.4, the critical concentration is 0.109 g cm^{-3}, and the critical temperature is 65.3 °C. The macroscopic behavior of phase separation is given by the coexistence curve, which in the neighborhood of the critical point shows a cubic dependence on the reduced temperature. The behavior of PEOX in water is expressed in terms of excess thermodynamic functions of dilution derived from osmometry and static light scattering. The low-temperature thermodynamics are shown to be consistent with the phase transition. Static light-scattering experiments show excess scattering at small angles concurrent with the appearance of slow relaxation modes in dynamic scattering. Both are consistent with long-range concentration fluctuations in PEOX–water solutions. The variety of measurements is consistent with the hypothesis that the system can experience partial organization at all temperatures, even well below the LCST, and that the origin of the organization is a specific hydrogen-bonded interaction between the carbonyl oxygen of PEOX and water.

I. Introduction

The work[1] here reported was initiated from previous investigations on the relation between the chemistry and physical behavior of aqueous solutions of polymers having a lower consolute solution temperature (LCST) or phase separation on heating. As reported,[2] these early studies provided a synthetic copolymerization scheme to produce polymeric films having a desired temperature dependence of solute transport property.

In this paper, we characterize the solution behavior of poly(2-ethyloxazoline) (PEOX[3]) in water. PEOX is an amorphous, nonionic, tertiary amide polymer with a repeat unit $-CH_2N(COC_2H_5)CH_2-$ and is prepared by the cationically initiated ring-opening polymerization of 2-ethyl-2-oxazoline.[4] The polymer exhibits[5] a broad range of solubility in polar organic solvents and behaves nearly as a Θ solute[6] in water at room temperature. The aqueous solutions undergo a liquid–liquid phase separation above 60 °C.

The solution properties of PEOX in water presented in the following sections are determined from osmometry, dynamic and static light scattering, and phase equilibria measurements. Osmometry and static light-scattering results are used to derive excess thermodynamic dilution functions.[7] These functions describe the interplay between the enthlapy and entropy of solution which controls the miscibility of PEOX in water. Insofar as data could be acquired, the low-temperature thermodynamic measurements are entirely consistent with, and predictive of, the LCST phase transition. The molecular origin for the thermodynamic behavior is in part related to specific interactions between water and PEOX, verified by infrared spectroscopy.

The macroscopic properties of the phase separation are described by the coexistence curve, which for multicomponent solutions (PEOX: M_w/M_n = 2.4) is appreciably different from the cloud point curve.[8] The critical behavior of the phase separation is described by a cubic dependence of the composition of the coexisting phases on the reduced temperature.[9]

Static light scattering in dilute solution is used to determine molecular weight and molecular size.[10] Dynamic scattering[11] is used to find translational diffusion coefficients and hydrodynamic radius. Static[12-17] and dynamic[18-26] scattering have demonstrated inhomogeneity in moderately to highly concentrated solutions of a variety of polymers and are applied here to solutions of PEOX. In this study, we show that the inhomogeneity arises from specific interactions between PEOX and water which contribute to partial organization at lower temperatures, and to the LCST phase transition at higher temperatures.

II. Materials and Methods

1. Materials. Poly(2-ethyloxazoline) was obtained from Dow Chemical Co. Aqueous solutions of PEOX were dialyzed prior to extensive ultrafiltration with constant stirring under nitrogen pressure in a Nucleopore ultrafiltration cell with a 100 000 molecular weight cutoff membrane. The filtered solution was thoroughly freeze-dried to constant weight. The residual ash content of purified polymer was negligible.

2. Experimental Technique. a. Osmometry. Osmotic measurements were performed on a Wescan Recording Membrane Osmometer, Model 231. The instrument as calibrated with a hydrostatic manometer showed a linear response up to 100 cm of hydrostatic pressure. Osmotic pressures were obtained by using a 5000 D cutoff membrane for concentrations up to ca. 0.10 g cm^{-3}.

Data were analyzed for the molecular weight and thermodynamic parameters by using eq 1 for the reduced osmotic pressure π/c:

$$\pi/c = RT/M_n + A_2c \quad (1)$$

where R is the gas constant, T is the absolute temperature, M_n is the number-average molecular weight, c is the polymer concentration (g cm^{-3}), and A_2 is the second virial coefficient (mol cm^3 g^{-2}).

b. Light Scattering. The light-scattering apparatus included a Malvern photon correlation system with 64 multibit channels (Model K7025), a temperature-controlled chamber (±0.02 °C), a goniometer-mounted photomultiplier with an analyzer and interference filters, a 15-mW helium–neon laser, a 5-W Argon ion laser, and a HP 9825 computer for data retrieval and analysis. The incident light intensity was monitored by partially reflecting the incident light onto a photodiode detector.

Solutions for light scattering were filtered through a combination of a prefilter and a 0.2-μm Millipore filter directly into a cylindrical quartz cell (1-cm i.d.) which was then covered tightly with a polymeric cap, all in a glovebox.

The cell was placed in the scattering vat filled with an aqueous solution of glycerol (80% v/v) as an index matching fluid. Two light-scattering methods were used to probe the solution behavior of PEOX in water.

0024-9297/90/2223-4688$02.50/0

i. Static Scattering. In dilute solutions, the excess Rayleigh ratio $\Delta R(\theta)$ ($=R(\theta)_{soln} - R(\theta)_{solv}$) due to concentration fluctuations at scattering angle θ was analyzed for molecular weight, thermodynamic parameters, and molecular size by using the expression[10]

$$Kc/\Delta R(\theta) = M_w^{-1}(1 + (qR_g)^2/3) + 2A_2c \quad (2)$$

where M_w is weight-average molecular weight, R_g is the radius of gyration, and $q = 4\pi n_0 \sin(\theta/2)/\lambda_0$ is the momentum transfer vector. Here, λ_0 is the wavelength in vacuum and n_0 is the refractive index of the solvent. The constant[27] K is given by $(2\pi n_0 \cdot (dn/dc))^2/N\lambda_0^4$ where N is Avogadro's number. The refractive index increment, dn/dc, of the solution was measured on a differential refractometer. For light scattering of PEOX in water at $\lambda_0 = 6328$ Å, $K = 1.97 \times 10^{-7}$ cm^2 mol g^{-2} if $n_0 = 1.3316$ (water) and $dn/dc = 0.165$ cm^3 g^{-1} are used.

The Rayleigh ratio, $R(\theta)$, is calculated[28] from

$$R(\theta) = C_R I(\theta) \sin\theta (n_s/n_c)^2/I_0 \quad (3)$$

where $I(\theta)$ is the instrument reading for scattered light, I_0 is that for incident light, and n_s and n_c are the refractive indices of the scattering solution and the calibration liquid. The factor $(n_s/n_c)^2$ is the refractive index correction for the volume viewed by the photomultiplier. The scattered intensities are photon counts recorded by the K7025 correlator. Toluene was used as a scattering reference to determine the constant C_R in eq 3. The Rayleigh ratio for toluene is $R_{V,V}(90°) = 10.5 \times 10^{-6}$ cm^{-1}. The subscripts correspond, respectively, to a vertically polarized incident light and to the vertical component of the scattered light collected by the detector through the analyzer. This value was derived from $R_{V,V+H}(90°)/(1 + \rho_V)$ where V+H signifies the collected total scattered light of both polarizations and ρ_V is the depolarization for scattered light. At 6328 Å, the value[29] $R_{V,V+H}(90°)$ is 14.02×10^{-6} cm^{-1} and ρ_V was measured as 0.329 for toluene. No depolarized scattering due to PEOX was observed in the concentration range reported in this paper.

Proper alignment[27] of the optical and detection system was verified by measuring in a dilute aqueous solution of rhodamine B (excited with 5140 Å) the fluorescence intensity, $F(\theta)$, at 6328 Å as a function of the observation angle θ. For isotropic fluorescence, the photomultiplier signal is proportional to the volume viewed which varies as $\sin^{-1}\theta$. Values of $F(\theta)\sin\theta/F(90°)$ plotted against θ were found to be independent of θ with deviations less than ±1% for a range of angles between 22° and 145°.

ii. Dynamic Scattering. The translational diffusion coefficient and the effective hydrodynamic radius of PEOX in water were determined in dilute solution by quasielastic light scattering. The experimental unnormalized homodyne autocorrelation function $C(q,t)$ was analyzed by using a three-parameter model

$$C(q,t) = H_0 + H_1 \exp(-2\Gamma(q)t) \quad (4)$$

in a nonlinear least-squares program. Γ is the average decay rate which depends on the momentum transfer vector q. Assuming homodyne scattering, the diffusion coefficient is $D = \Gamma/q^2$. Except for verification of the angular dependence of $\Gamma(q)$, the majority of experiments were obtained at 90° scattering angle. Sample times were chosen so that the accumulated correlation function covered 2–3 times the apparent exponential decay.

In cases where the autocorrelation function was a sum of two exponentials, two decay constants could be extracted by judicious choice of sampling times in several separate experiments on each sample, so long as the two decay rates were separated by several orders of magnitude. At temperatures approaching the phase transition, it became necessary to discard some of the initial data points (1–5 points) in the long time correlation function since these points contain information on the short (fast) time correlation function. The baseline for the short correlation functions was the asymptotic value attained for a function covering two to four relaxation times. The delayed baseline was used for long-time correlation functions. Similar results were obtained from separate experiments and from fitting using multiple component exponential regressions at intermediate sampling times.

c. Phase Diagram. i. Cloud Point Curve. The cloud point curve was obtained by raising the temperature of homogenous solutions of known concentration of PEOX in water until optical scattering was observed. By use of a Perkin-Elmer 300 spectrophotometer equipped with a digital temperature controller and a heating chamber modified to accept a 1-mm path length cell, the temperature for phase separation was taken as that at which the optical density at 6328 Å changed by 0.05 unit when heating at a constant rate of 0.1 °C/min.

ii. Coexistence Curve. The coexistence curve was obtained by raising the temperature of solutions in small increments above the critical temperature. The coexistence curve is a plot of these increments against the concentration of the two separated phases. Phase separations were carried out in sealed vials filled with approximately 4 mL of solution. Vials, placed in a carousel holder, were immersed in an insulated temperature-controlled bath (±0.02 °C). Temperature increments were measured with a differential thermometer. After temperature equilibration, the samples were left in the bath undisturbed until phase separation was completed (24–48 h). Aliquots from each of the two phases were collected with gas-tight syringes, and the concentration of each phase was determined on a differential refractometer.

d. Refractive Index. A differential refractometer of the Brice type[30] was used to determine the refractive index and concentration of PEOX solutions. The refractive index of aqueous solutions of sodium chloride[31] was used for calibration. For concentration measurements, the refractometer was calibrated against known concentrations of PEOX in water ranging from 0.001 to 0.20 g cm^{-3}.

e. Viscometry. Viscosity was measured with a Cannon-Fenske viscometer calibrated at two temperatures with freshly distilled water. The intrinsic viscosity, $[\eta]$, for PEOX in water is 46.5 cm^3 g^{-1} at 30 °C.

f. Density Measurement. Densities of the solutions, ρ, were determined with a pycnometer for a concentration range up to ca. 0.15 g cm^{-3} in the temperature range from 30 to 60 °C. These measurements were used to find the partial molar volume of water in solution and to convert the polymer volume concentration, c_p, to volume fraction, ϕ_p, by using[32]

$$\phi_p = 1/[1 + (v_0/v_p)(\rho/c_p - 1)] \quad (5)$$

with v_0 the specific volume of the water and v_p that for PEOX, measured[6] as 0.877 cm^3 g^{-1} at 25 °C.

g. Infrared Spectra. Solutions of PEOX were prepared as 0.01 g cm^{-3} at various molar ratios of deuterated acetonitrile and deuterium oxide. The spectra were taken on a Perkin-Elmer 580B dispersive spectrometer in a 0.1-mm path length BaF_2 cell against a suitable reference cell.

III. Results

1. Thermodynamic and Solution Characteristics. The solution properties and molecular parameters of PEOX in water at several temperatures are summarized in Table I. In Figure 1, the reduced osmotic pressure is linear in concentration well into the concentrated solution region of PEOX (ca. 0.05 g cm^{-3}). Second virial coefficients derived from analysis of light scattering in dilute solutions (<0.01 g cm^{-3}) are in good agreement with osmotic results. The second virial coefficients (Figure 2) show that water is a thermodynamically good to moderate solvent for PEOX only at 30 °C.

The molecular size of PEOX in water can be determined from the slope of the reduced scattered intensities, $c/\Delta R(\theta)$, versus $\sin^2(\theta/2)$ extrapolated to zero concentration (eq 2). In dilute solutions between 30 and 45 °C, $c/\Delta R(\theta)$ was within experimental error independent of the scattering angle. Hence $qR_g \ll 1$ in eq 2, indicating that PEOX in water behaves as an isotropic scatterer. This result places an upper limit to R_g at $\lambda/20 = 240$ Å.

Table I
Solution and Molecular Properties of PEOX (M_w/M_n = 2.4)

method	mol wt	temp, °C	$A_2 \times 10^4$, mol cm^3 g^{-2}	R_g, Å	R_h, Å	solvent
osmometry	4.92×10^4 (M_n)	30	8.56			H_2O
		45	3.66			
		60	-1.46			
static scatter	11.6×10^4 (M_w)	30	8.74	<240[a]		H_2O
		40	5.41			
		60	-1.28			
dynamic scatter		30			107[b,c]	H_2O
viscosity		30		111[d]		H_2O
osmometry		30	11.77			EtOH
static scatter		30	12.20	154		EtOH
dynamic scatter		30			124[c]	EtOH

[a] PEOX is an isotropic scatterer, i.e., $qR_g \ll 1$ in eq 2. An upper limit for R_g is 6328 Å/(1.3316 × 20). [b] Hydrodynamic radius, evaluated from eq 13, is temperature independent between 30 and 57 °C. [c] Derived from zero concentration diffusion coefficient. [d] Radius of gyration estimated from eq 6: $[\eta]$ = 46.5 cm^3 g^{-1} at 30 °C with M_w = 116 000.

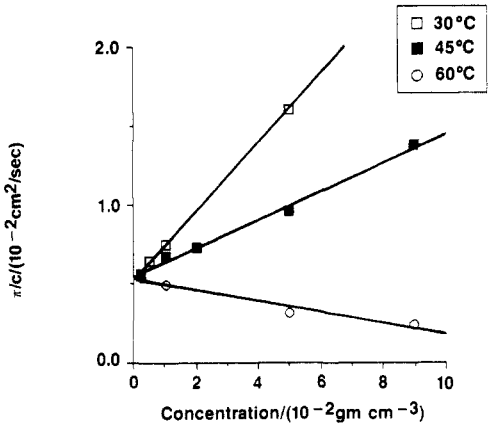

Figure 1. Reduced osmotic pressure, π/c, vs concentration of PEOX in water at 30, 45, and 60 °C. The solid lines were generated from a least-squares fit of the data to eq 1.

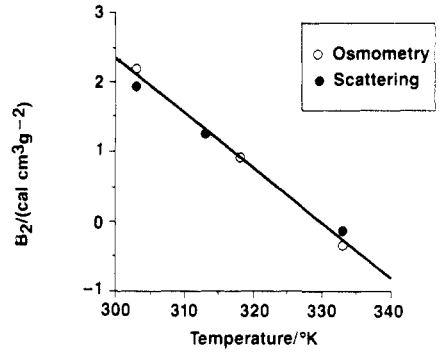

Figure 2. Temperature dependence of the second virial coefficients, $B_2 = RTA_2$, derived from osmometry (○) and static light scattering (●). The Θ temperature where B_2 = 0 is 56 °C and $B'_2 = (dB_2/dT)$ = -0.019 cal cm^3 g^{-2} K^{-1}.

We estimated R_g from intrinsic viscosity using the expression[33,34]

$$[\eta] = \Phi 6^{3/2} R_g^3 / M_w \quad (6)$$

We calculated R_g to be 111 Å using $\Phi = 2.68 \times 10^{23}$ mol^{-1} and $[\eta]$ = 46.5 cm^3 g^{-1} at 30 °C.

The virial coefficients of Table I were used to calculate the excess chemical potential of the solvent, $\Delta\mu_1^E$, given by[7]

$$\Delta\mu_1^E = \Delta h_1^E - T\Delta s_1^E \approx -B_2 c^2 V_1 \quad (7)$$

where

$$\Delta h_1^E = (B'_2 T - B_2) c^2 V_1 \quad (8)$$

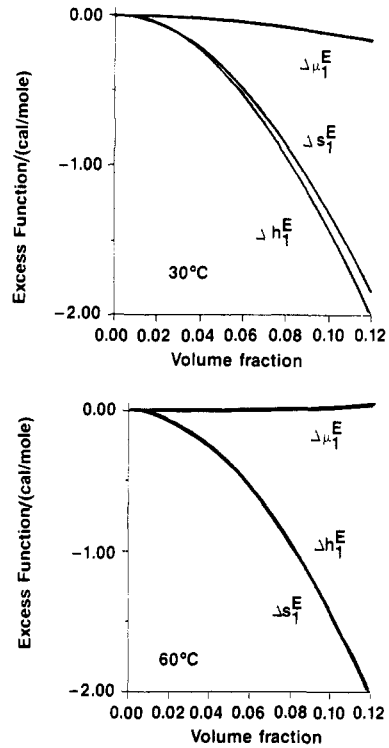

Figure 3. Excess thermodynamic dilution functions chemical potential $\Delta\mu_1^E$, enthalpy of mixing Δh_1^E, and entropy of mixing Δs_1^E plotted against volume fraction of PEOX in water for 30 °C (top) and 60 °C (bottom).

$$\Delta s_1^E = B'_2 c^2 V_1 \quad (9)$$

are the excess enthalphic and entropic dilution components, respectively. Here $B_2 = RTA_2$, $B'_2 = dB_2/dT$, and V_1 is the partial molar volume of water. The excess functions represent the behavior of the solution relative to that described by the ideal solution

$$\Delta\mu_1^{id} = -T\Delta s_1^{id} = -B_1 c V_1 \quad (10)$$

and

$$\Delta h_1^{id} = 0 \quad (11)$$

with $B_1 = RT/M_n$. From the temperature dependence of B_2, given in Figure 2, we obtained a solution Θ temperature (B_2 = 0) of 56 °C and B'_2 = -0.019 cal cm^3 g^{-2} K^{-1}. The excess functions plotted against the volume fraction of PEOX are shown in Figure 3 for 30 and 60 °C.

2. Phase Diagrams. The cloud point and coexistence curves plotted against concentration of PEOX are given in Figure 4. The coexistence curve was obtained at the critical concentration (0.109 g cm^{-3}) determined by the

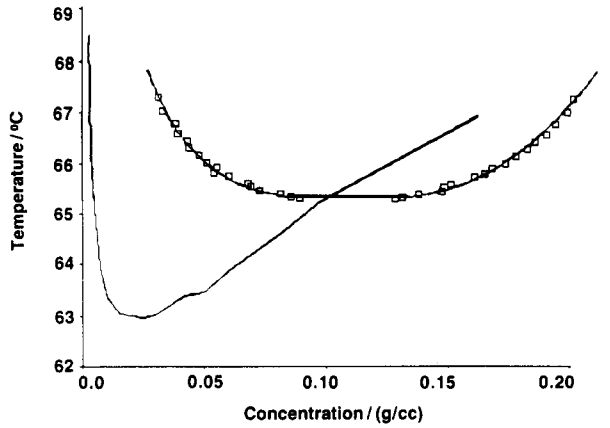

Figure 4. Cloud point (isolated solid curve) and coexistence curve (squares) for PEOX in water for M_w = 116 000 as a function of concentration. The coexistence curve was determined at the critical volume fraction of 0.097 (0.109 g cm^{-3}). The solid curve associated with the coexistence data is eq 12b.

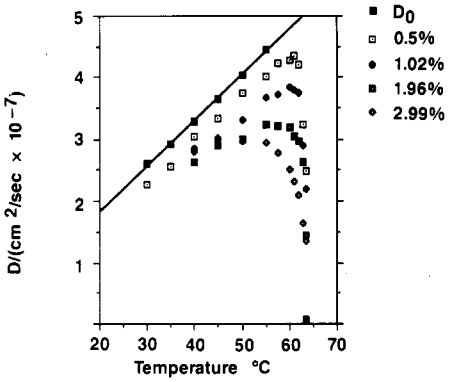

Figure 5. Low-concentration temperature dependence of diffusion coefficients of PEOX in water at 90° scattering angle for several concentrations. The solid line connects points which are the diffusion coefficients at zero concentration.

phase volume method.[35] The concentrations of the coexisting phases were measured over a 2-deg range above the critical temperature, T_c.

The relation between the volume fractions of the two coexisting phases, ϕ^+ and ϕ^-, at temperature T is summarized by[9]

$$\delta\phi = |\phi^+ - \phi^-| = 2\phi_c B_c \epsilon^\beta \qquad (12a)$$

where the reduced temperature is $\epsilon = (T - T_c)/T_c$ and ϕ_c (=0.097) and β are the critical volume fraction and exponent, respectively. The data were least-squares fitted over a 2-deg temperature range. The best fit was found with T_c = 338.3 K, β = 0.33 ± 0.02, and B_c = 4.4 ± 0.3. To fully accord with the data to the extent shown in Figure 4, a modification of eq 12a is necessary

$$\phi^{+/-} = \phi_c + 1.363\epsilon \pm \delta\phi/2 \qquad (12b)$$

where $\phi^{+/-}$ is either ϕ^+ or ϕ^-, the coexisting volume fractions.

3. Dynamic Light Scattering. The temperature dependence of the diffusion coefficient, D, at low concentrations of PEOX in water is given in Figure 5. The diffusion coefficient increases with temperature at low temperatures as 1/viscosity of water but decreases above the Θ temperature (56 °C). This decrease in D may be interpreted as a slowing down of the concentration fluctuations as the LCST is approached.

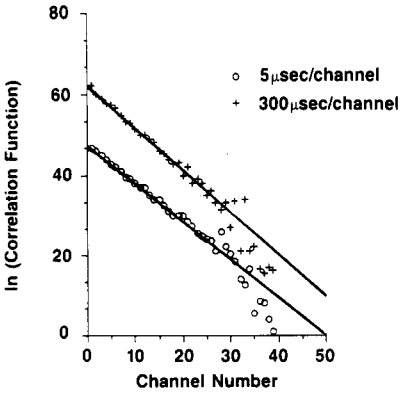

Figure 6. Plots of the logarithm of the correlation function vs correlator channel number for 0.099 g cm^{-3} of PEOX at 40 °C, for sampling times of 5 and 300 μs. These plots are also typical of the data obtained at concentrations higher than 0.05 g cm^{-3}.

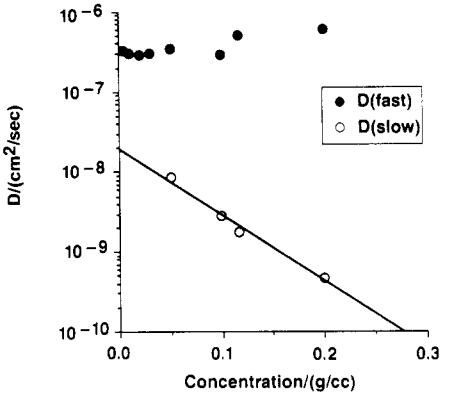

Figure 7. Concentration dependence of the diffusion coefficients from the fast (solid circles) and slow (open circles) relaxation modes of PEOX at 45 °C.

The hydrodynamic radius, R_h, of PEOX was calculated from the Stokes–Einstein relation

$$R_h = k_B T/(6\pi\eta_0 D_0) \qquad (13)$$

where k_B is Boltzmann's constant and η_0 is the viscosity of water. The translational diffusion coefficient at zero concentration, D_0, was obtained by extrapolating the diffusion coefficients to zero concentration (see Figure 5) by using data determined at concentrations less than 0.03 g cm^{-3} at temperatures between 30 and 56 °C. A constant R_h = 107 Å was found for this temperature range.

Above 63 °C, two relaxation modes were obtained at all concentrations, each of which showed an exponential decay profile. Two distinct correlation functions were also observed in high concentrations of PEOX at all temperatures. In Figure 6, the logarithm of representative correlation functions is plotted against the correlator channel number for 0.099 g cm^{-3} PEOX to illustrate the exponential profiles seen.

The separation between the two modes depends on concentration, temperature, and scattering angle. The slow-mode diffusion coefficient, which shows a strong dependence on concentration ($\approx 1/c^2$), may be separated from the fast-mode diffusion coefficient by several orders of magnitude as illustrated in Figure 7. This separation, however, decreases as the temperature approaches the phase transition (Figure 8). The decay constant Γ (eq 4) for both modes was apparently proportional to q^2 and intercepted the origin, consistent with pure diffusive processes.

At low temperatures, the slow-mode correlation function could not be found for a freshly filtered solution until a

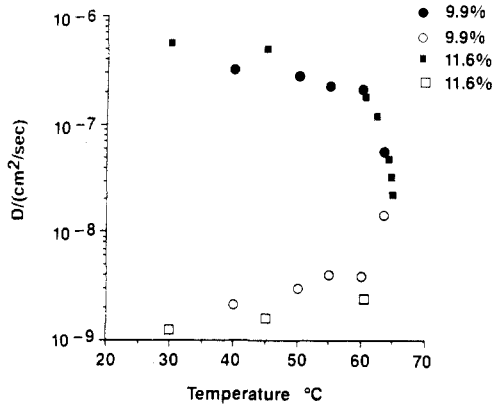

Figure 8. Temperature dependence of the diffusion coefficients for the fast (solid markers) and slow (open markers) relaxation modes of PEOX in water at concentrations of 0.099 g cm^{-3} (circles) and 0.116 g cm^{-3} (squares).

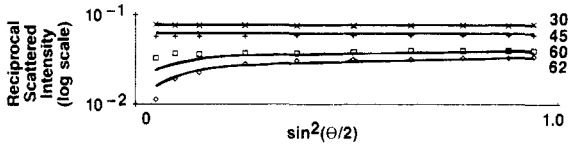

Figure 9. Plots of the log of the reduced excess scattered intensities from static scattering experiments, $c/\Delta R(\theta)$ (eq 2) vs $\sin^2(\theta/2)$ for 0.0094 g cm^{-3} of PEOX at the indicated temperatures. These plots typify the behavior of scattered intensities for dilute solutions. The solid lines are drawn with the ad hoc eq 17 discussed in the text. The numerical scale is such that toluene has a value of unity.

sufficient period of time (on the order of 5–15 min) had elapsed. After the delay, a gradual increase in the forward scattering intensity was observed with a corresponding development of the correlation signal. There was no difficulty in recording the fast-mode decay immediately after filtration. Within experimental error, the fast-mode diffusion coefficients did not change with time. Because of the low amplitude of the slow mode, the kinetic evolution could not be followed. Similarly, the proportionality of the slow diffusion coefficient to q^2 should be considered tentative.

4. Static Light Scattering. Temperature effects on the distribution of scattered light with angle are given in Figure 9 for 0.0094 g cm^{-3} PEOX. These plots are representative of the behavior found in dilute solution and illustrate the near independence of $c/\Delta R(\theta)$ with $\sin^2(\theta/2)$ at low concentration for temperatures below 60 °C. The non-zero slope develops as the temperature is raised with excess low-angle scattering becoming strongly evidence at 62 °C.

Excess low-angle scattering is observed at higher PEOX concentration at all temperatures. Figure 10 shows the reciprocal scattered intensities for 0.116 g cm^{-3} PEOX on a logarithmic scale as a function of $\sin^2(\theta/2)$. The solid lines in this figure are drawn from

$$I = I_0[(1 + \xi_1^2 q^2)^{-1} + (1 + \xi_2^2 q^2)^{-1}] \quad (14)$$

where

$$\xi_1 = 3.74\ \text{Å}/((T - T_c)/T_c)^{2/3} \quad (15)$$

$$\xi_2 = 2800\ \text{Å}$$

$$I_0 = 0.026((T - T_c)/T_c)^{5/4} \quad (16)$$

with T_c = 338.8 K. The fit with these parameters has a maximum error of 16%. The rms error value of $(I - I_m)/I_m$, where I_m are the data in Figure 10, is estimated as less than 2 times the experimental error.

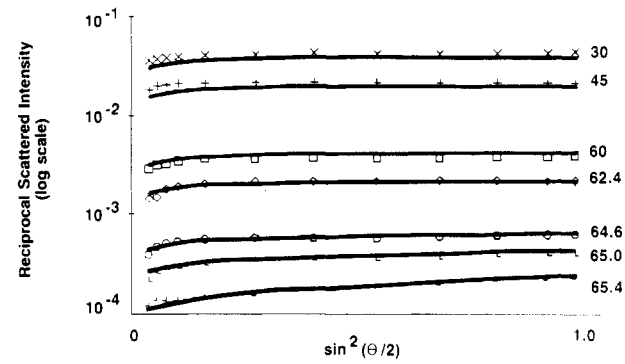

Figure 10. log of the reduced scattered intensity vs $\sin^2(\theta/2)$ at 0.116 g cm^{-3}. The solid lines are described by eq 14.

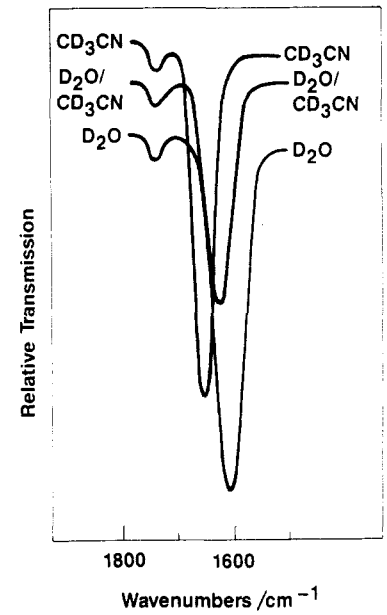

Figure 11. Infrared spectra at room temperature of 0.01 g cm^{-3} PEOX in 100% CD_3CN, in 100% D_2O, and in 1:1 mole ratio of CD_3CN/D_2O.

The form of the first term in eq 14 is the conventional Ornstein–Zernike scattering expression.[9,36] The exponents in eqs 15 and 16, taken from ref 37, are consistent with the phase separation results. The term in eq 14 involving ξ_2 is arbitrarily chosen to be of the same form as that involving ξ_1 but incorporates the observed temperature independence.

The solid lines in Figure 9 are an ad hoc modification of eq 14 to include concentration effects:

$$I/I_0 = C_N^{0.02}[(1 + \xi_1^2 q^2)^{-1} + (1/C_N)((T/T_c)^{8/C_N})(1 + \xi_2^2 q^2)^{-1}] \quad (17)$$

where $I_0 = 0.026((T - T_c)/T_c)^{1.25C_N^{1/2}}$, $C_N = 0.0094/0.116$ (the concentration ratio). Equation 17 has not been resolved with eq 2.

5. Infrared Spectra. Figure 11 shows the infrared spectra of PEOX between 1500 and 1800 cm^{-1} at selected molar ratios of CD_3CN and D_2O. These spectra show the effects of the solvent environment on the position of the carbonyl stretching frequency. The frequency shifts from 1648 cm^{-1} in a polar, non-hydrogen-bonding solvent (100% CD_3CN) to 1609 cm^{-1} in a hydrogen-bonding solvent (100% D_2O).

IV. Discussion

LCST systems present the anomaly that as the system is heated and the overall entropy is increased, the system

seems to become more organized, that is, of lower entropy. The thesis put forth is that in fact parts of the system—the macroscopic phase separation—do become more organized, but the "lost" entropy appears in the solvent component in the low-density phase by virtue of the breaking of hydrogen bonds between the polymer and the solvent.

1. Thermodynamic and Phase Behavior. The solution behavior of PEOX in water can be described with the excess thermodynamic dilution functions.[38,39] A negative $T\Delta s_1^E$ can be realized in solutions where specific interactions, such as dipole–dipole or hydrogen bonding, are effective in imposing constraints on the relative distance and orientation between unlike components of the mixture. These interactions are contributive factors for observing a lower consolute solution temperature below the boiling point of the solvent.[40] Hydrogen-bonding interaction between PEOX and water is substantiated from infrared spectra which show a preferential interaction between water and the carbonyl oxygen of PEOX. This finding corresponds with results found between nonpolymeric amides and water,[41] where the enthalpy and entropy of formation for hydrogen bonding have been determined.[42,43]

At 30 °C, we find that $|\Delta h_1^E| > T|\Delta s_1^E|$ and $\Delta\mu_1^E$ makes a negative contribution to the chemical potential of the solvent $\Delta\mu_1 = \Delta\mu_1^{id} + \Delta\mu_1^E$ where $\Delta\mu_1^{id} < 0$ at all temperatures. The solubility of PEOX in water is dominated by the more favorable energy contribution ($\Delta h_1^E < 0$) which overcomes the unfavorable entropic contribution ($-T\Delta s_1^E > 0$). At 60 °C, $T|\Delta s_1^E|$ is slightly greater than $|\Delta h_1^E|$ and $\Delta\mu_1^E$ makes a positive contribution to $\Delta\mu_1$. At these higher temperatures, the increased mobility of the interacting molecules tends to lessen the effectiveness of the specific interaction. This is shown by the progressive decrease of the solvent property of water as reflected by the temperature dependence of the second virial coefficient B_2 (Figure 2). Finally, if the water–water or PEOX–PEOX energy of interaction is relatively more favorable than the water–PEOX interaction, the entropy loss in solution will not be sufficient to keep the components mixed, and the free energy of the system is lower through separation into high- and low-concentration solutions of polymer.

Unlike a binary solution, where the cloud point and the coexistence curves are identical, the cloud point curve for a polydispersed polymer in a single solvent does not fully describe the macroscopic behavior of phase separation.[8] Concentrations corresponding to points on the cloud point curve connected with a horizontal line at a given temperature are not coexisting phases derived from a phase separation. It has been shown,[8,44] however, in polymer solutions that one of the coexisting phases resides on a curve (called a shadow curve) which is not amenable to direct observation. Furthermore, the two branches of the coexistence curve converge as the composition of the solution approaches the critical concentration. To obtain a coexistence curve like that shown in Figure 4, the overall polymer concentration must be in the neighborhood of the critical concentration.[44]

The critical exponent $\beta = 0.33$ for the PEOX–water system is in good agreement with values found for binary liquids of small molecules[45] and for the polystyrene–cyclohexane,[46] system which has an upper consolute solution temperature (UCST). The critical exponents found in these systems lie between 0.33 and 0.35. This agreement indicates that β is fairly independent of the system since the same value is obtained in the polystyrene–cyclohexane UCST system and the PEOX–water LCST system. The universality of the critical exponent is supported by the favorable comparison of β with those obtained from one-component systems.[47]

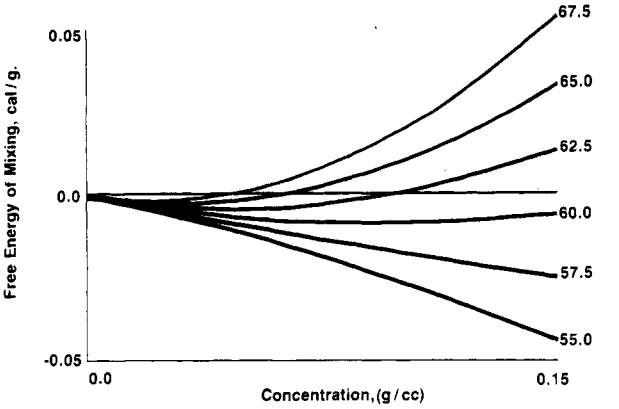

Figure 12. Calculated free energy of mixing as a function of concentration for the system PEOX–water assuming second-order functions of concentration for both osmotic pressure and density. The origin of the calculations is set out in Appendix 1. That the curves rise above zero free energy at finite concentration beyond 60 °C is consistent with the coexistence curves of Figure 4.

2. Consistency of Thermodynamic Measures and Phase Transition Data. During the course of the investigations reported here, we frequently posed the question, Is the observed phase transition consistent with the thermodynamic measurements made below the transition temperature? An affirmative answer would permit the argument that all of the phenomena observed are manifestations of the same set of interactions.

Classical solution[48] theory gives a description for the total free energy of a solution from osmotic data, as outlined in Appendix 1. To make use of the classical theory, the osmotic and density data were fitted to empirical polynomials, and the composite set of equations was solved and converted to Fortran by using MACSYMA.[49] The results are shown in Figure 12.

A complete free energy versus concentration curve for a system which would spontaneously separate would have a hump in the center: an initial concentration in the central region would segregate into higher and lower concentrations to yield lower overall free energy. The segregated solutions would then be the coexistence curve. While osmotic data could not be acquired at polymer concentrations high enough to reproduce the entire free energy vs concentration curve, we judge that Figure 12 is consistent with the left branch of the coexistence curve, Figure 4, within the experimental and mathematical accuracy permitted by the data. We therefore conclude that the low-temperature thermodynamic data and the LCST phase transition are self-consistent.

3. Light Scattering. Light-scattering experiments show that the excess scattering at low angles in static scattering coincide with the appearance of a second relaxation mode in dynamic scattering. Both observations in solutions of PEOX in water are consistent with large-scale concentration fluctuations which are controlled by the temperature and concentration of the solution.

Both static and dynamic light scattering can be written in terms of a thermodynamic parameter, the osmotic derivative, $\partial\pi/\partial c$ ($\propto \partial\Delta\mu_1/\partial c$). While this term can qualitatively account for some of the temperature behavior demonstrated by D and $c/\Delta R(\theta)$, it does not provide information on the angular distribution of scattered light or on the existence of a slow relaxation mode. Excess scattered intensities similar to those of PEOX solution a few degrees from the phase transition have also been

observed in other polymer–solvent systems.[12,15,17,50-52] The appearance of a slow relaxation mode in dynamic scattering in the accompaniment of excess low-angle scattering seems to be associated with the development of long-range spatial and temporal concentration fluctuations[36] that would eventually drive the system toward a macroscopic phase separation.

In concentrated PEOX solutions, the large-scale fluctuations persist at all temperatures and are described with two Ornstein–Zernike like terms. The unusual component of the scattered light in eq 14 is that described by the term $(1 + \xi_2^2 q^2)$, where ξ_2 is independent of temperature. The form of this term was chosen in the spirit of the Ornstein–Zernike model, where a short-range direct correlation function can effectively produce a long-range concentration correlation.[9] ξ_2, which has the unit of length, is about 20 times larger than the molecular dimension of the PEOX in water. Since this component is not observed at low concentrations and appears to be independent of absolute scattered intensity, we conclude that the term describes solution inhomogeneity arising from PEOX–water interactions. The structures of this inhomogeneity are not given by the present analysis. However, excess scattering in other polymer–solvent systems, some of which do not exhibit a phase transition, has been associated with inhomogeneity due to special orientation between polymer molecules[12-14] or to aggregation[16,17] or to polydispersity.[53,54]

The intensity of scattered light, being proportional to the static structure factor, is the Fourier transform of the concentration correlation function.[55] The expression for the structure factor can be inverted to yield the concentration correlation function. Without knowing what intermolecular interactions underlie the static structure factor, it is clear that the statistics of the static light scattering require fluctuations on two different length scales.

The findings at high temperature and high concentration are supported by eq 17, the extension of eq 14, to include concentration effects. The parameters in eq 17 with dimension of length are the same as eq 14. The effect of concentration is in the relative weighting of the two scattering modes.

The inhomogeneity of solutions seen in static scattering is qualitatively substantiated by the presence in dynamic scattering of the slow relaxation mode. The appearance of this mode is observed in conjunction with an increase in the forward scattered intensity following filtration. Correlation lengths estimated from the Stokes–Einstein equation using the measured viscosity are 2–3 times smaller than those determined from static light scattering, but still much larger than molecular dimensions.

Slow modes have been found in concentrated solutions in other polymer–solvent systems.[24,26,56] These modes have been associated with the self-diffusion coefficient of the polymer as a whole in a random network of other polymers[19,23] and which at infinite dilution corresponds to translational diffusion of polymer in solvent. Since we were unable to detect slow relaxation modes below 0.05 g cm^{-3}, we cannot determine if the slow mode diffusion coefficients extrapolate to the zero concentration diffusion coefficients of the fast mode shown in Figure 5.

4. Ethanol and D_2O as Solvent. Ethanol, which is a better solvent than H_2O (as shown in Table I), does not show phase separation at any temperature below the boiling point at atmospheric pressure. This observation suggests intramolecular interactions are not a major driving force for the phase transition. Use of D_2O in place of H_2O yielded a cloud point some 3 °C lower. This lowering of the transition temperature by 3 °C with D_2O seems to parallel the relationship between the critical temperature of H_2O and D_2O.[57] Together with the infrared results, the effectiveness with which the LCST of PEOX can be modified by substituting D_2O for H_2O strongly supports the existence of hydrogen bonding between PEOX and water.

V. Summary

The thermodynamic properties of dilute solutions of PEOX in water have been characterized by osmometry, static and dynamic light scattering, and phase equilibria experiments. The properties found are in accord with behavior for systems possessing a lower consolute phase transition and are consistent with specific interactions associated with hydrogen bonding between water and the carbonyl oxygen of PEOX.

The light-scattering experiments show excess scattering at small angles in static scattering and the concurrent appearance of a slow relaxation mode in dynamic scattering. Both are consistent with long-range concentration fluctuations in PEOX–water solution which exist in solutions near the phase transition temperature and in concentrated solutions at all temperatures.

Acknowledgment. We gratefully acknowledge the substantial efforts of Mr. R. Seeg in many of the measurements reported here and the many discussions with our colleagues in these laboratories. We thank the Polaroid Corp. for permission to publish this work.

Appendix. An Expression for the Total Free Energy of Mixing of a Solution Using Second-Order Expansions for Osmotic Pressure and Solvent Density

The total free energy of mixing of a two-component solution is

$$\Delta g_m = \phi_1 \Delta\mu_1 + \phi_2 \Delta\mu_2$$

where ϕ_1 and ϕ_2 are the volume fractions of the solute and solvent and $\Delta\mu_1$ and $\Delta\mu_2$ are the chemical potentials. The volume fraction of the solute is

$$\phi_2 = 1/[1 + 0.877\rho_w(\rho_w/C - 1)]$$

where ρ_w is the density of water, $\phi_1 = 1 - \phi_2$, C is concentration, and 0.877 is the specific density of PEOX. The chemical potential of the solute is calculable from the osmotic pressure data:

$$\Delta\mu_1 = -(B_1 C + B_2 C^2)(M_w/\rho_w)$$

where M_w is the molecular weight of water, $\pi(C) = (B_1 + B_2 C)C$, and B_1 and B_2 are first-order polynominals in temperature. $\Delta\mu_2$ can be expressed in terms of concentration as

$$\Delta\mu_2 = P\int_{1/\upsilon_p}^{c} \phi_1/\phi_2(\partial\Delta\mu_1/\partial C)\, dC$$

where υ_p is the specific density of PEOX and P is the degree of polymerization taken as the ratio of molecular weights. For computational purposes, we describe the density of the solutions as an empirical polynomial

$$\rho_s = \rho_w(X_0 + X_1 C + X_2 C^2)$$

The above equations were integrated by using MACSYMA. The final expression, with the additional translation $B_1 C$

$+ B_2C^2 = \pi$, is

$$\Delta g_m = -(B_1CPM_w\rho_wX_0V_p^3 \ln (C^6V_p^6) + ((6CM_w^2\pi + (4B_2C^4 + 3B_1C^3)pM_w)\rho_wX_1 + (6CP + 6C)M_w\pi\rho_wX_1 + ((12p + 6)M_w\pi - 12B_1CPM_w)\rho_wX_0 + (-6CP - 6C)M_w\pi)V_p^3 + (-6B_1CPM_w\rho_wX_1 - 12B_2CPM_w\rho_wX_0 + 6B_1CPM_w)V_p^2 + (-3B_1CPM_w\rho_wX_2 - 6B_2CPM_w\rho_wX_1 + 6B_2CPM_w)V_p - 4B_2CPM_w\rho_wX_2)/(6C\rho_w^2V_P^4 + (6C^2\rho_w^2X_2 + 6C\rho_w^2X_1 + 6\rho_w^2X_0 - 6C\rho_w)V_p^3)$$

References and Notes

(1) Some of the results were presented at the 1982 IUPAC 28th Macromolecular Symposium.
(2) Taylor, L. D.; Cerankowski, L. D. *J. Polym. Sci., Polym. Chem. Ed.* **1975**, *13*, 2551.
(3) PEOX, a trademark of Dow Chemical.
(4) Frump, J. A. *Chem. Rev.* **1971**, *71*, 483.
(5) Ginter, S. P.; Huffines, D. Technical Bulletin; Dow Chemical Company.
(6) Chiu, T. T.; Thill, B. P.; Fairchok, W. J. In *Water-Soluble Polymers*, Glass, J. E., Ed.; Advances in Chemistry 213; American Chemical Society: Washington, DC, 1986; pp 425–433.
(7) Schulz, V. G. V.; Cantow, H. J. *Elektrochem. Z.* **1956**, *60*, 517.
(8) Koningsveld, R.; Staverman, A. *J. Kolloid Z. Z. Polym.* **1976**, *218*, 114.
(9) Stanley, H. E. *Introduction to Phase Transition and Critical Phenomenon*; Oxford University Press: New York, 1971.
(10) Evans, J. M. In *Light Scattering from Polymer Solutions*; Huglin, M. B., Ed.; Academic Press: London, 1972; pp 89–164.
(11) Berne, B. J.; Pecora, R. *Dynamic Light Scattering*; Wiley: New York, 1976.
(12) Dautzenberg, H. *J. Polym. Sci., Polym. Symp.* **1972**, *39*, 123.
(13) Dautzenberg, H. *J. Polym. Sci., Polym. Symp.* **1977**, *61*, 83.
(14) Hyde, A. J. In *Light Scattering from Polymer Solutions*; Huglin, M. B., Ed.; Academic Press: London, 1972; pp 385–396.
(15) Koberstein, J. T.; Picot, C.; Benoit, H. *Polymer* **1985**, *26*, 673.
(16) Strazeille, C. *Makromol. Chem.* **1968**, *119*, 50.
(17) Polik, W. F.; Burchard, W. *Macromolecules* **1983**, *16*, 978.
(18) Brown, W.; Johnson, R. M.; Stilbs, P. *Polym. Bull.* **1983**, *9*, 305.
(19) Brown, W. *Macromolecules* **1984**, *17*, 66.
(20) Brown, W. *Macromolecules* **1985**, *18*, 1713.
(21) Brown, W. *Macromolecules* **1986**, *19*, 1083.
(22) Balloge, S.; Tirrell, M. *Macromolecules* **1985**, *18*, 817.
(23) Amis, E. J.; Han, C. C. *Polym. Commun.* **1982**, *23*, 1403.
(24) Amis, E. J.; Janmey, P. A.; Ferry, J. D.; Yu, H. *Macromolecules* **1983**, *16*, 441.
(25) Amis, E. J.; Han, C. C.; Matsushita, Y. *Polymer* **1984**, *25*, 650.
(26) Mathiez, P.; Mouttet, C.; Weisbuch, G. *J. Phys. (Les Ulis, Fr.)* **1980**, *41*, 519.
(27) Utiyama, H. In *Light Scattering from Polymer Solutions*; Huglin, M. B., Ed.; Academic Press: London, 1972; pp 61.
(28) Einaga, Y.; Mitani, T.; Hashizume, J.; Fujita, H. *Polym. J. (Tokyo)* **1979**, *11*, 565.
(29) Kaye, W.; McDaniel, J. B.; *Appl. Opt.* **1974**, *13*, 1934.
(30) Brice, B. A.; Hawler, M. *J. Opt. Soc. Am.* **1951**, *41*, 1.
(31) Kruis, Z. *Z. Physik. Chem.* **1936**, *34B*, 13.
(32) Koningsveld, R.; Staverman, A. J. *J. Polym. Sci., Polym. Phys. Ed.* **1968**, *6*, 325.
(33) Flory, P. J.; Fox, T. G. *J. Am. Chem. Soc.* **1951**, *73*, 1994.
(34) Pyun, C. W.; Fixman, M. *J. Chem. Phys.* **1966**, *44*, 2107.
(35) Koningsveld, R.; Staverman, A. J. *J. Polym. Sci.* **1967**, *16C*, 1775.
(36) Ornstein, L.; Zernicke, F. *Proc. Acad. Sci. Amsterdam* **1914**, *17*, 793.
(37) Kawahara, N.; Fenby, D. V.; Tamsky, M.; Chu, B. *J. Chem. Phys.* **1971**, *55*, 1140.
(38) Malcolm, G. N.; Rowlinson, J. S. *Trans. Faraday Soc.* **1957**, *53*, 921.
(39) Prigogine, I.; Defray, R. *Chemical Thermodynamics*, Longmans: London, 1965.
(40) Hirschfelder, D. H.; Stevevson, D.; Erying, H. *J. Chem. Phys.* **1937**, *5*, 896.
(41) Kobayashi, M.; Kobayashi, M. *J. Phys. Chem.* **1980**, *84*, 781.
(42) Henson, D. B.; Swenson, C. A. *J. Phys. Chem.* **1973**, *77*, 2401.
(43) Takahashi, F.; Li, N. C. *J. Am. Chem. Soc.* **1966**, *88*, 1117.
(44) Rehage, G.; Moller, D.; Ernst, O. *Makromol. Chem.* **1965**, *88*, 232.
(45) Stein, A.; Allen, G. F. *J. Phys. Chem. Ref. Data* **1973**, *2*, 443.
(46) Nakata, N.; Kuwahara, N.; Kaneko, M. *J. Chem. Phys.* **1975**, *62*, 4278.
(47) Levelt Sengers, J. M. H.; Straub, J.; Vicentini-Missoni, M. *J. Chem. Phys.* **1971**, *54*, 5034.
(48) Kurata, M. Thermodynamics of Polymer Solutions; Harwood Academic Publishers: New York, 1982.
(49) MACSYMA is a proprietary software package from SYMBOLICS, Inc.
(50) Einaga, Y.; Ohashi, S.; Tong, Z.; Fuijta, H. *Macromolecules* **1984**, *17*, 527.
(51) Cuniberti, C.; Bianchi, U. *Polymer* **1974**, *15*, 346.
(52) McIntyre, D. M.; Wims, A.; Green, M. S. *J. Chem. Phys.* **1962**, *37*, 3019.
(53) Benoit, H. *J. Polym. Sci.* **1953**, *11*, 507.
(54) Benoit, H.; Holtzer, A. M.; Doty, P. *J. Phys. Chem.* **1954**, *58*, 635.
(55) Chen, S. H. In *Physical Chemistry: An Advanced Treatise*; Henderson, D., Ed.; Academic Press: New York, 1971; pp 85–156.
(56) Nishio, I.; Wada, A. *Polym. J. (Tokyo)* **1980**, *12*, 145.
(57) Eisenberg, D.; Kauzmann, W. *The Structure and Properties of Water*; Oxford University Press: New York, 1969.